Recent Advance of Transition-Metal-Based Layered Double Hydroxide Nanosheets: Synthesis, Properties, Modification, and Electrocatalytic Applications

Huan Yi, Shiyu Liu, Cui Lai, Guangming Zeng,* Minfang Li, Xigui Liu, Bisheng Li, Xiuqin Huo, Lei Qin, Ling Li, Mingming Zhang, Yukui Fu, Ziwen An, and Liang Chen*

Nowadays, to alleviate the growing pressure of energy shortages and environmental pollution, electrochemical energy conversion is seen as a fossil-free, secondary pollution-free, and highly efficiency pathway. Electrocatalysts, as the "heart" of the electrochemical conversion process, play a key role in accelerating reaction rates and promoting efficiency. Transition-metal-based layered double hydroxides (TM LDHs), one of the famous electrocatalysts, show unique 2D supermolecular-stratified structure, excellent electronic properties, and their raw materials are easily available. In this review, electrocatalysis-related properties of TM LDHs and the state-of-the-art synthesis methods of TM LDH-based electrocatalysts are summarized. Modifications for promoting the development of TM LDH-based electrocatalysts are included, such as carbon materials modification, defect engineering, and noble metal loading. Then, the application of TM LDH nanosheets in the field of electrocatalysis is reviewed in detail. Finally, recent challenges, ongoing improvements, and future expectations for TM LDH nanosheets are presented.

1. Introduction

With the continuous consumption of limited resources and deterioration of the environment,[1] electrochemical conversion systems become the spotlight because of their potential in energy conversion and storage.[2] For these electrochemical conversion processes, electrocatalyst plays a key role in speeding up the reaction rate, improving the reaction performance and enhancing the reaction selection and sensitivity.[3] However, the electrocatalysts used in practical commercial applications are basically rare metal-based materials, especially Pt-, Ir-, and Ru-based materials. To achieve the sustainable development of economy and industrialization,[3c,4] efficient and low-cost nonrare metal-based electrocatalysts are being explored to replace these high-cost rare electrocatalysts.

By the virtue of low cost, abundant precursor sources, high catalytic activity and stability, 2D transition-metal-based layered double hydroxide (TM LDH) nanosheets have invoked a great deal of researcher's interest lately.[5] Most of TM LDHs are synthetic layered nanomaterials (including host layer metal ions and interlayer anions), possessing flexible tunability of chemical composition and adjustable character of structure. And the manufacture process is simple and low cost. Based on these, TM LDH nanosheets are a promising electrocatalyst for new energy development. Plenty of experiments and theoretical studies have proved that TM LDH nanosheets showed excellent catalytic performance for various electrochemical conversion reactions, such as oxygen evolution reaction (OER),[6] hydrogen evolution reaction (HER),[7] and oxygen reduction reaction (ORR).[8] And the electrocatalytic activity of some modified TM LDH nanosheets can be comparable to that of noble metal based electrocatalysts.[9]

The number of publications about TM LDHs in energy and environmental science has been increasing all the time.[10] Li and co-workers overviewed the catalytic application of TM LDHs with focusing on LDH-based catalysts and LDH-based catalysts support.[11] Long et al. kept an eye on the tailored strategy,[12] effects of metal combinations,[13] and crystal engineering[14] of TM LDHs. The reviews on energy application of TM LDHs mostly focused on energy storage like battery and supercapacitor.[15] Lately, the OER of 2D TM LDHs was specially concluded for not only energy storage but also new energy production, attracting a lot of attention owing to the 2D nanostructure and unique properties.[16] Nevertheless,

---

Dr. H. Yi, Dr. S. Liu, Prof. C. Lai, Prof. G. Zeng, Dr. M. Li, Dr. X. Liu,
Dr. B. Li, Dr. X. Huo, Prof. L. Qin, Dr. L. Li, Dr. M. Zhang, Dr. Y. Fu, Dr. Z. An
College of Environmental Science and Engineering
Hunan University
Changsha, Hunan 410082, China
E-mail: laicui@hnu.edu.cn; ZGMing@hnu.edu.cn

Dr. H. Yi, Dr. S. Liu, Prof. C. Lai, Prof. G. Zeng, Dr. M. Li, Dr. X. Liu,
Dr. B. Li, Dr. X. Huo, Prof. L. Qin, Dr. L. Li, Dr. M. Zhang, Dr. Y. Fu, Dr. Z. An
Key Laboratory of Environmental Biology and Pollution Control
(Hunan University)
Ministry of Education
Changsha, Hunan 410082, China

Prof. L. Chen
Faculty of Life Science and Technology
Central South University of Forestry and Technology
Changsha, Hunan 410004, China

The ORCID identification number(s) for the author(s) of this article can be found under https://doi.org/10.1002/aenm.202002863.

DOI: 10.1002/aenm.202002863

apart from OER, other electrocatalytic applications of 2D TM LDHs with high industrial and academic importance are also worth reviewing, such as HER for H_2 yield, two-electron ORR for H_2O_2 production, CO_2 reduction (CO_2RR) to generate CO as "green" fuels, N_2 reduction (NRR) to produce NH_3, and selective redox of organics to form value-added products. A few reviews focused on these aspects of the 2D TM LDH nanosheets. Even if these contents are involved, it is not complete. An update on the development of TM LDH nanosheets with emphasizing nanostructure is absent. Certainly, a systematic analysis on the underlying reasons of improved electrocatalytic performance is in demand to explore the structure–performance correlation. This timely review comprehensively summarizes the latest progress in synthesis, modification, mechanism, application for "green" energy, and the facing challenges of TM LDH nanosheets for further advances.

In this work, we focus on the synthesis and modification of 2D TM LDH nanosheets, as well as their applications in electrocatalysis. We begin with a briefly description of the atomic and crystal structure to show the construction of LDHs. Subsequently, the electrochemical related properties of LDHs that need to be considered when designing TM LDH-based electrocatalysts materials are summarized, including the tunability of chemical composition and structure, and the adjustable electronic properties. Then, the state-of-the-art synthesis and modification methods (including carbon nanomaterials modification, defect engineering and noble metal loading) of TM LDH nanosheets are concluded with investigating the principle, which plays a leading role in the next improvement and innovation of preparation. At last, OER, HER, ORR, and other important electrocatalytic applications (i.e., CO_2RR, NRR, and selective redox of organics) of versatile TM LDH nanosheets are discussed in detail (**Figure 1**).

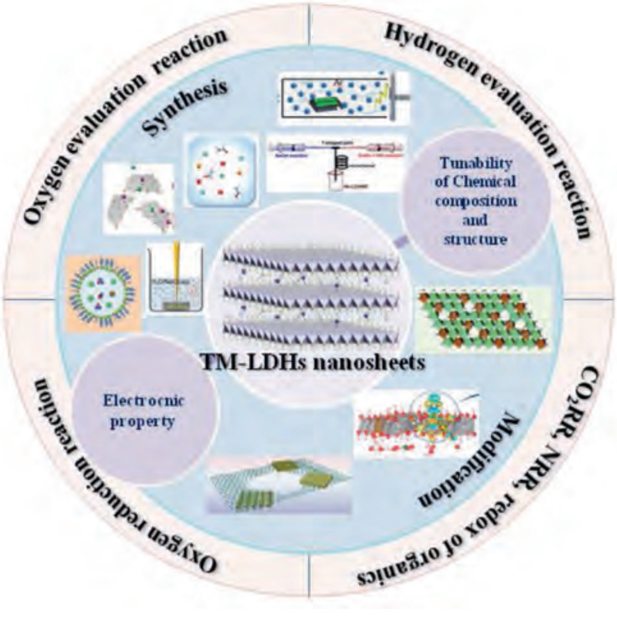

Figure 1. The illustration of the synthesis, properties, modification and electrocatalyst applications of TM LDH nanosheets.

2. Atomic and Crystal Structure of TM LDH Materials

TM LDHs, a class of anionic clays with supermolecular structure, are composed of positive charge host layers and match-able interlayer guest anions.[12,15] The crystal structure unit of host layer is edge-sharing metal hydroxide octahedron constructed by the coordination of a central metals (mainly includes divalent metal cations M^{2+} and trivalent metal cations M^{3+}) and six hydroxide groups. The molar ratio (X) of $M^{2+}/(M^{2+} + M^{3+})$ is a key factor for crystallization formation. The interlayer anions (A^{n-}) contain inorganic anions and organic substances, such as CO_3^{2-}, SO_4^{2-}, HPO_4^{2-}, OH^-, Cl^-, NO_3^-, sodium dodecyl sulfonate (SDS), etc. TM LDHs are expressed as $[M^{2+}{}_{1-x}M^{3+}{}_x(OH)_2](A^{n-})_{x/n}\cdot mH_2O$, while the value of x is supposed to between 0.2 and 0.33. The close combination of the host layers and match-able interlayer guest anions depends on two aspects: I) the electrostatic interactions between the center metal cations and interlayer anions; II) the hydrogen bond binding forces between the oxhydryl and interlayer anions. With the decrease of M^{3+} contents, the positive charge density of host layers decreases, which reduce the electrostatic interactions between the center metal cations and interlayer anions. Moreover, the organic anion-intercalated TM LDHs possess a larger interlayer spacing than the inorganic anion-intercalated ones.[17]

The chemical composition of TM LDHs can be tuned by adjusting the ratio of M^{2+}/M^{3+} and the type of metal cations or interlayer anions. Different chemical composition leads to different structure. Generally, when the radius of metal cations with two different valence states (M^{2+} and M^{3+}) are similar, the host layers are formed easily.[15a] **Table 1** shows the radius of metal cations and the effective combinations of different metal cations to form TM LDHs. Additionally, the stability of TM LDHs host layers is directly related to the collocation of metal cations in different valence states.

The performance of TM LDHs in electrochemical reaction is restricted by solid state diffusion. Enlarging interlayer space can accelerate the kinetics of electrochemical reactions to reduce the restriction.[18] Larger interlayer spacing favors the electron transfer and mass transfer via providing more space to allow adequate electrolyte participate in reaction. Because of the relatively weak interlayer bonding between host layer and interlayer guest anions, TM LDHs show remarkable ability to exchange the interlayer anions. Introducing large ion into the TM LDHs interlayer can increase the interlayer spacing.[10a,b] Zeng et al. chose two different inorganic anions (CO_3^{2-} and NO_3^-) to design NiCo LDH–CO_3^{2-} and NiCo LDH–NO_3^- electrocatalysts with different interlayer spacing.[19] The electrocatalytic activity was positively correlated with interlayer spacing and the order was NiCo LDH–NO_3^- > NiCo LDH–CO_3^{2-} > NiCo hydroxide.[19] The interlayer spacing of TM LDHs with common inorganic anions intercalations is summarized as follows: OH^- (7.55 Å) < CO_3^{2-} (7.65 Å) < F^- (7.66 Å) < Cl^- (7.86 Å) < Br^- (7.96 Å) < I^- (8.16 Å) < NO_3^- (8.79 Å) < SO_4^{2-} (8.58 Å) < ClO_4^- (9.20 Å). Generally, the interlayer spacing increases with the increase of radius size. Expect inorganic anions, a lot of organic substances were also used to replace the common anions to enlarge interlayer spacing.[10c,d,16,18,20] Zhong et al. selected SDS as interlayer

Table 2. A summary of research with enlarging LDH interlayer spacing.

Composition of LDH	Interlayer anion	Interlayer spacing [Å]	BET surface area [m^2 g^{-1}]	Application	Efficiency	Ref.
NiAl–LDH	Sodium oleate	*d*-Spacing of 43.7 Å	86.37	As electrode for aqueous asymmetric supercapacitor	High energy density of 40.26 Wh kg^{-1} at a power density of 943 W kg^{-1}	[18]
NiCo–LDH	CO_3^{2-}	7.58		Urea oxidation electrocatalysis		[19]
	NO_3^-	8.60			86%	
NiFe–LDH	Sodium dodecyl sulfonate	24.9	62.35	Electrocatalyst toward OER	Onset overpotential of 289 mV and a Tafel slope of 39 mV dec^{-1}	[20]
NiFe–LDH	Borate ion	6.2	170.9	Electrocatalyst toward OER	Onset overpotential of 270 mV and a Tafel slope of 42 mV dec^{-1}	[93]
NiCo–LDH	Sodium					
dodecylbenzene sulfonate	15.3	15.28	As electrode for supercapacitor	1094 F g^{-1} at a scan rate of 5 A g^{-1}		[92a]
CoFe–LDH		11.3	165.2	As electrode for supercapacitor	175 F g^{-1} at 2 A g^{-1}	[92b]
ZnCo–LDH		9	116.4	Electrocatalyst toward OER	0.375 V at the current density of 2 mA cm^{-2} and Tafel slope of 101 mV dec^{-1}	[92c]
CoFe–LDH	NO_3^-	7.5		As anode for sodium ion batteries	First discharge capacity of 498 mAh g^{-1} and a charge capacity of 328 mAh g^{-1} at 1 A g^{-1}	[92d]
NiFe–LDH		9.5		Electrocatalyst toward OER	Overpotential of 203 mV and a Tafel slope of 39 mV dec^{-1}	[92e]
NiMn–LDH		*d*-Spacing of 8.6 Å	50.2	Electrocatalyst toward OER	Overpotential of 0.35 V, a Tafel slope of 40 mV dec^{-1}	[92f]

Different TM-based chemical components endow TM LDHs with diverse electronic structures. Gao et al. studied the electronic structures of four kinds of LDH nanosheets with different TM (CoFe–, CoNi–, NiFe–, and ZnCo–LDHs) by using density functional theoretical (DFT) calculation.[29] And the role of electron-spin polarization in electrocatalytic performance over the four TM LDHs was also studied. The observed obvious spin polarization behavior could boost the electrons transfer.[29] All four TM LDHs showed small bandgap. Among them, ZnCo–LDHs possessed relatively large bandgap that was dominated by the d atomic orbitals of Co, which led to the highest occupied molecular orbital and lowest unoccupied molecular orbital, indicating the lack of obvious electron transfer in ZnCo–LDHs. Correspondingly, ZnCo–LDH nanosheets also showed weaker electron conductivity, and finally performed lower electrocatalytic activity.

Changing the surface structure of LDHs with fixed chemical composition can also tailor the electronic structure of LDHs to gain higher electrocatalytic efficiency. Surface distortion can also generate d-electron delocalization, which can improve the electron transfer efficiency between electrocatalysts and reactants, thereby further decreasing the adsorption energy of the electrochemical reaction.[30] The existence of electron delocalization can be proved by the delocalized spin states of active atoms.

Additionally, the existence of defects can adjust the electronic structure of the LDH-based electrocatalysts, such as oxygen vacancy and metal vacancy. Since the function of unoccupied bonding t_{2g} orbitals of MO_6 center (MO_{6-x}), LDHs with oxygen vacancies present high electronic conductivity and excellent capacity adsorption for oxygen-related intermediates.[31] For metal vacancy, due to the diversity of electron and orbital distributions of the metal atoms, the absence of metal atoms could increase the valence state of adjacent metal centers.[31]

Ions regulation has been proved to be an effective method to tune the electronic structure, such as anionic doping/replacing.[32] Huang et al. introduced sulfion, an anion with polarization property, into CoAl–LDHs (**Figure 2**a).[33] Sulfion regulation can adjust the ion-covalent properties by the formation of the Co—O bonds and Co—S dangling bonds, which favors to tune the electronic structure around these active sites. Sun et al. presented that interlayer anions replacing can affect the electronic structure of the exposed surface metal atoms of TM LDH nanosheets.[34] More electrons can be transported from the interlayer anions with low redox potential (like hypophosphites) to the hydroxide layers, while less electrons transfer from anions with high redox potential (like fluorion) (Figure 2b,c). More electrons transfer would increase the electron density and maintain high-valence states of metal sites.

4. Synthesis and Modifications

4.1. Synthesis of TM LDH Nanosheet

As mentioned in Section 2, the unique structure of TM LDHs shows highly layer charge density, which makes the preparation of TM LDH nanosheets more difficult than that of other layered materials by exfoliation methods (belonging to top-down methods). The usually adopted exfoliation method is liquid exfoliation, which is always accompanied by the assistance of ultrasonication. As time goes by, various top-down methods were explored to synthesis TM LDH nanosheets, like plasma etching,[26] which can greatly reduce the preparation time.

induced by binder. Additionally, Wang et al. found that nitrogen plasma exfoliate methods can produce the abundant vacancies, and introduced N atom into CoFe LDHs ultrathin nanosheets (Figure 10b):[26] bulk CoFe LDHs were first prepared via hydrothermal process, and then bulk CoFe LDHs was exfoliated (treating by N_2 plasma) to generate ultrathin N-doped CoFe LDH nanosheets. The doping of N atoms adjusted the electronic density of nearby active sites (Co and Fe atoms) and thus enhanced the absorption ability of hydrogen- and oxygen-based intermediates.

Structure Distortion and Grain Boundary or Lattice Disorder: Beside vacancies and doping, researchers excavated many other defect manufacture methods to modify LDHs, such as dislocation, grain boundary and lattice disorder.[27,30,82] Chen et al. developed an inorganic-organic hybrid intermediate-assisted liquid-exfoliation method to introduce structure distortion, and then delocalize the spin states of Ni for Ni-based compound.[30] The delocalized spin states enhanced the electronic conductivity and provided low adsorption energy for reaction intermediates. Zhou et al. reported a flame-engraved method to prepare NiFe–LDHs with abundant defects:[27] NiFe LDHs array was first synthesized via hydrothermal process, and then was engraved by butane inner flame (≈500 °C). The lattice plane (110) of the synthesized NiFe–LDHs showed visible hexagonal hole due to the accumulation of oxygen vacancies and other defects.[27] Gao and Yan reported a precipitation process to fast prepare monolayer CoFe– and NiFe–LDH nanosheets within 5 min.[29] Plentiful defects and lattice distortion were formed in the synthesized LDH nanosheets. Spin-polarization of Fe-based LDH with abundant defects accelerated the electron transfer.[29] Yin et al. used the molecular precursor of metal and carbon sources to synthesize amorphous NiFe LDH nanosheets based electrocatalyst with lattices distortion via one-pot solution process (Figure 10c).[82]

4.2.3. Noble Metal Loading

In addition to above methods, noble metal loading was also employed to improve the electrocatalytic performance of TM LDH nanosheets.[83] Noble metal nanoparticles have outstanding electronic conductivity and robust physicochemical stability.[84] The electrons can rapidly transfer from noble metals to the active sites of TM LDHs, improving the adsorption ability of oxygen-containing intermediate reactants (OH*, O*, and OOH*).[85] Generally, chemical reduction and electrodeposition are used to load noble metals.[85–86]

Chemical reduction method requires adding reductant, like borohydride and alcohols. Anantharaj et al. used borohydride as the reductant to synthesize a Pt NPs/NiFe–LDH nanosheets composite:[87] first, NiFe–LDH nanosheets were prepared via hydrothermal method, and then Pt ions was reduced on NiFe LDHs. The addition of Pt NPs roughened the surface of NiFe–LDH nanosheets, providing efficient and intimate access of ECSA to the reactants. Apart from the strategy of evenly dispersing precious metals on the surface of LDH nanosheets, noble metals can be inserted into the interlayer area of LDH nanosheets.[88] For example, Ma et al. also used chemical reduction method with ethylene glycol and triethanolamine as the reductant to synthesize in situ grown metallic Ag^0 intercalated CoAl LDHs.[88] This composite showed enlarged interlayer space, augmented ECSA and higher electronic conductivity.

Electrodeposition method shows the advantage on the accurate introduction of trace of noble metal into TM LDH nanosheets synthesis. Guo et al. developed a two-step synthesis strategy to synthesize the Pd–NiFe LDH nanosheets: NiFe LDH nanosheets were first fabricated on nickel foam via hydrothermal process and subsequently Pd was electrodeposited on NiFe LDHs.[89] Similarly, Wan et al. adopted a three-step method containing hydrothermal reaction, phosphorization and electrodeposition process to construct the FeNiP@CoNi–LDH nanosheet nanoarrays vertically grown on CC.[86b] Moreover, Zhang et al. used electrodeposition method to load single-atom Au on NiFe LDHs successfully.[85] Compared with nanometer-scaled noble metals, single-atom metals loading show the following merits: Au usage will lessen and the atomic utilization can be maximized.

Different modification methods fit different electrocatalytic applications. CNMs modification can solve the limit of TM LDH nanosheets in electrochemical conversion reaction: relatively low electronic conductivity and decreased ECSA caused by the nanosheets agglomeration, and it is cost efficient. CNMs modified TM LDH nanosheets can show good electrocatalytic activity not only in OER, but also in HER and ORR, because I) CNMs act as the support for TM LDH nanosheets to prevent the agglomeration, II) the specific defect types in CNMs could be the active sites for OER, HER, or ORR, and III) CNMs, showing excellent electronic conductivity, can transfer the electrons in reaction to promote the electrochemical performance. Defect engineering, including vacancy, doping, structure distortion and grain boundary or lattice disorder, is often used to greatly improve the electrocatalytic OER activity of TM LDH nanosheets in a direct way with tuning the electronic structure and exposing more active sites. The exposed active sites capture those intermediate reactive substances, and attract metal atoms to form new structure and generate new active sites. Noble metal loading was commonly adopted to construct bifunctional or multifunction TM LDH-based electrocatalysts for OER, HER and so on. The loaded noble metals can rapidly capture and transfer the electrons to the active sites of TM LDHs. The addition of noble metals adjusts the electronic state of active sites (metals and O species in LDHs), accelerated charge transfer, and provided more active sites introduced by defects and lattice distortion, thus enhancing the adsorption capacity toward H and oxygen-containing intermediate reactants (OH*, O*, and OOH*) to enhance the contact of active sites and reactants, and accelerating the Volmer step kinetics. The related electrocatalytic applications of modified TM LDH nanosheets were detailed described in Section 5.

5. Electrocatalytic Application of Transition-Metal-Based LDH Materials

5.1. Oxygen Evolution Reaction

Unquestionable, the efficiency of energy storage system (e.g., water splitting, fuel cells, and metal–air batteries), largely

Table 6. The ORR performance of TM LDH nanosheets reported in literature.

Composition of LDHs	Electrode	Electrolyte	Loading [mg cm^{-2}]	Binder	η_{onset} [V]	Tafel slop [mV dec^{-1}]	ECSA/C_{dl} [mF cm^{-2}]	Ref.
NiCo$^{\text{III}}$Fe–LDH/NGO	GC	0.1 м KOH		Ethanol and Nafion	0.880		3.240	[8]
NiFe–LDH/Co, N–CNFx	GC	0.1 м KOH	0.12	Nafion	0.790			[69]
NiRu–LDH/Ti_4O_7	GC	0.1 м KOH	0.12	Nafion and isopropanol	0.800	58		[106a]
NiFe–LDHs/rGO	RDE	1.0 м KOH	0.18	Ethanol and Nafion	0.796			[96]
CoMn–LDH@CNT	RDE	0.1 м KOH	1.1–1.7	Ethanol and Nafion	–0.274		12.6	[107b]
MCN$^{\text{c}}$/NiFe–LDH	RDE	0.1 м KOH	0.4	Ethanol and Nafion	0.900	46	12.6	[67b]
nNiFe–LDH/3D MPC	RDE	0.1 м KOH	2.0	Nafion and isopropyl alcohol				[107a]
Ag–CoAl LDHs	RDE	0.1 м KOH	0.35	Nafion	0.765	109	0.364	[88]

C_{dl}: electrochemical double-layer capacitances; ECSA: electrochemically active surface area; MCN: metal–organic framework derived carbon network; RDE: rotating disk electrode.

positive charge host layers that is favorable for oxygen adsorption, TM LDH nanosheets based materials exhibit excellent stability and high density active sites for ORR[67b,69,96,107] (**Table 6**). According to the previous researches, TMs with oxidation state are the mainly activity sties for ORR, especially Ni, Fe, Co and Mn. Therefore, TM LDHs/carbon hybrids including Ni, Fe, Co and Mn atom were fabricated. For example, Zhou et al. prepared a NiCo$^{\text{III}}$Fe–LDH/N-GO hybrid, which was a versatile electrocatalyst for ORR/OER owing to the exposure of more active sites introduced by high valence Co and N doping.[8] Duarte and co-workers proposed a CoMn–LDH@CNT, which showed a similar electrocatalytic efficiency for ORR to the Pt/C catalyst.[107b] The incorporation of CNT_HNO_3 increased the ECSA for CoMn–LDH@CNT and improved the electron transfer, thus enhancing the ORR activity. These common ORRs with H_2O as the final products are four-electron process.

Electrocatalytic two-electron ORR is a potential technology to replace the present anthraquinone process for distributed small-scale H_2O_2 production.[108] Huang et al. fabricated Ni–LDHs/carbon nanosheets as electrocatalyst to produce H_2O_2 and generate electricity in a metal–air fuel cell.[109] DFT calculation indicated that the most enlarged edge Ni sites of small size Ni–LDH chips played a key role to promote the conversion of O_2 to H_2O_2, and the steric effect of carbon nanosheets inhibited the decomposition of H_2O_2 and the dissociation of O—O bond to suppress the occurrence of four-electron pathway ORR. The Ni–LDHs/carbon nanosheets showed impressive performance for H_2O_2 production via a two-electron pathway (5239.67 mmol h^{-1} g$_{\text{cat.}}$$^{-1}$).

5.4. Other Electrocatalytic Applications

In addition to exhibit splendid electrocatalytic activity for OER, HER, and ORR, TM LDH nanosheets also bloom in other electrocatalytic applications, such as CO_2RR, NRR, and redox of organic molecules. The electrochemical CO_2RR/NRR converts CO_2/N_2 to value-added products, contributing to long-term seasonal energy storage and cost-effective manufacture.[110] An N-doped LDH derived NiZnAl oxide was synthesized on reduced graphene oxide substrate (N-NiZnAl LDH/rGO) for electrocatalytic CO_2RR to produce CO:[111] one electron transferred to CO_2 to generate $CO_2^{\bullet-}$ active sites ($CO_2^{\bullet-*}$); subsequently, one electron and two protons further reduced $CO_2^{\bullet-*}$ to CO*; and then CO was desorbed from the N-NiZnAl LDH/rGO electrocatalyst. These steps can be summarized by Equations (1)–(3)

$$CO_2\,(aq) + e^- + * \rightarrow CO_2^{\bullet-*} \tag{1}$$

$$CO_2^{\bullet-*} + e^- + 2H^+\,(aq) \rightarrow CO^* + H_2O \tag{2}$$

$$CO^* \rightarrow CO + * \tag{3}$$

The kinetic rate of Equation (1), representing the first electron transfer, plays the key role in CO_2 electroreduction. Ji and co-workers proposed a hierarchical hollow nanotube of NiFeV–LDHs@CoVP for nitrogen electroreduction to ammonia.[112] The hierarchical structure increased the ECSA and exposed more active sites, and the strong chemical interaction between CoVP– and NiFeV–LDHs accelerated the electron transfer, which benefited the NRR process. **Figure 15** shows the associative (distal) pathway for NRR over NiFeV–LDHs@CoVP.[112] During the electrocatalytic process, charge in NiFeV–LDHs@CoVP transferred from TMs to nonmetal sites. N_2 was first adsorbed on positively charged metals, while negatively charged surface sites (P sites) anchored H^+ via hydrogen bonding, then the activated H^+ attacked the N triple bonds to form N—H bonds, and finally NH_3 was generated through the incorporation of H^+ and electrons step by step. Compared with industrial NH_3 production via Haber–Bosch process, electrocatalytic NRR does not require high temperature, high pressure, and H_2.

Due to the abundance of hydroxyl groups on the surface, TM LDH nanosheets exhibit good adsorption properties to organic molecules. Hence, TM LDHs are also widely used in the redox reaction of organic molecules, like renewable biomass-derived 5-hydroxymethylfurfural (HMF). Usually, HMF oxidation needs high temperature, high pressure, and dangerous reducing gas. Fortunately, thin TM LDH nanosheets have great potential to overcome the difficulties. NiFe–LDH nanosheets grown on CFP that showed excellent electrocatalytic performance on HMF oxidation under ambient conditions, and 98% selectivity of value-added 2,5-furandicarboxylic acid (FDCA) can be obtained in 10 h at 1.23 V$_{\text{RHE}}$.[113] Subsequently, a Cu_xS@NiCo–LDH core–shell nanoarray electrocatalyst was prepared, and it

Table 7. Summary on active sites and mechanism of TM LDH nanosheets for different electrocatalytic applications reported in literature.

Application	TM LDHs	Active sites	Mechanism	Ref.
OER	S-doped NiCoFe–LDH nanosheets	Ni(Co) oxyhydroxide active species transformed from Ni—S and Co—S bonds	3D hierarchical porous nanosheets provided highly exposed active sites and sulfur doping enhanced electrical conductivity.	[53c]
	Pt–NiFe–LDHs	Highly crystalline sheets, more conductive $Ni_{0.6}Fe_{2.4}O_4$ phases, Pt at certain concentrations	The shape selective synthesis and high degree of crystallinity enhanced the performance	[87]
	CoO/CoFe–LDHs	Co^{III} sites	The charge transferred from Co^{II} in the oxide to Fe^{III} through the interfacial Co—O—Fe bond, leading to abundant high valence Co^{III} sites.	[2d]
	NiCo–LDH nanosheets	Open coordination sites located along the edges	The open frameworks opened up more inner surface accessibility to the electrolyte ions and facilitate the fast mass transport and oxygen diffusion.	[59]
	CoFe–LDH/rGO	Co and Fe species	The shortened ion transport distance in the nanoscale dimension, and the broader interlayer space enhanced mass transfer. rGO with well-interconnected conductive networks enhanced the conductivity.	[64]
	NiFe–LDH nanosheets	Defects, Ni, Fe	Fe^{3+}/Ni^{2+} cation-exchange process endows LDH surfaces with nanoporous and abundant defects.	[76]
	Mn^{2+}-doped NiFe–LDHs	Ni, Fe, oxygen vacancies	Introducing Mn^{2+} with weaker electronegativity to Ni and Fe formed electron-rich structure of both Ni^{2+} and Fe^{3+} sites, fewer amount of –OH coordinated with Ni and Fe sites, leading to oxygen vacancies.	[79]
HER	Pt–NiFe–LDHs	Pt NPs	The shape selective synthesis and high degree of crystallinity enhanced the performance.	[87]
	Cu@NiFe LDH	Abundant exposed edges leaved by the few-layer NiFe LDH nanosheets vertically grow on the Cu nanowires, active sites in the 3D core–shell structures.	3D hierarchical nanoarchitecture with large surface areas, fast electron transport, and open channels for effective gas release enhanced OER activity.	[100a]
	CoFe–LDH@GDY	Fe 3d acted as electron-rich center, Co 3d band played as electron-depletion channel.	The incorporation with graphdiyne increased the number of catalytically active sites, enhanced charge transfer and prevented corrosion, leading to greatly enhanced electrocatalytic activity for OER and HER.	[77]
	NiFeRu–LDHs	Ru atoms that substituting Fe centers	The introduction of Ru atoms into NiFe–LDH efficiently reduced energy barrier of the Volmer step.	[7]
	NiFe LDH/CeOx	Oxygen vacancy sites	Oxygen vacancy increased the free charge carrier concentration, and benefited the absorption of H_2O molecules.	[98]
ORR	$NiCo^{III}Fe$–LDH/NGO	Ni and Fe sites	Dual-active-site mechanism: 1) Ni and Fe sites with electron-rich structure enhanced the OER activity. 2) The pyridinic-N and graphic-N in N-GO altered the electron density of carbon atoms to have a positive impact on the adsorption of O_2 and the breaking of O—O bonds in the ORR process.	[8]
	Ni-LDH C/CNSs	Ni edge sites located on CNSs/Ni-LDH	The steric effect of carbon nanosheets inhibited the decomposition of H_2O_2 and the dissociation of O—O bond to suppress the occurrence of four-electron pathway ORR.	[109]
CO_2RR	N-NiZnAl LDH/rGO	The doped N, the rich interface between NiO and ZnO particles	One electron transferred to CO_2 to generate $CO_2^{\bullet-}$ active sites ($CO_2^{\bullet-*}$); subsequently, one electron and two protons further reduced $CO_2^{\bullet-*}$ to CO*; and then CO was desorbed	[111]
NRR	NiFeV–LDHs@CoVP	Ni, Fe, Co, V active sites and P active sites	N_2 was first adsorbed on positively charged metals, while negatively charged surface sites (P sites) anchored H^+ via hydrogen bonding, then the activated H^+ attacked the N triple bonds to form N—H bonds, and finally NH_3 was generated through the incorporation of H^+ and electrons step by step.	[112]
Redox reaction of HMF	NiFe–LDH nanosheets	Fe^{3+} has a higher activity than Fe^{2+}	The introduction of Fe could increase the amount of active sites and enhance the catalytic activity.	[113]

I) More efforts are needed to excavate the fundamental science of the electrocatalytic efficiency of TM LDH nanosheets, such as the relationship between chemical composite/structure and electrocatalysis properties/activity; the accurate identification of electrocatalytic active sites and the nature action of different reaction active sites and the synergism between them. Uncertain actives sites affect the mechanism study. And mechanism investigation of electrochemical reaction is always based on DFT theoretical calculations, which is difficult to comprehensively analyze all the influencing factors. The chemical reaction process is dynamic and full of many uncertain factors. More in situ characterization and tracer technique should be developed to obtain real-time observation, and promote the study of the reaction transformation processes, especially the transformation of active sites.

S. Y. Liu, C. Zhang, G. M. Zeng, D. L. Huang, L. Qin, X. G. Liu, H. Yi, R. Z. Wang, F. L. Huang, B. S. Li, T. Y. Hu, *ACS Sens.* **2018**, *3*, 2566.

[4] a) F. Lyu, Q. Wang, S. M. Choi, Y. Yin, *Small* **2019**, *15*, 1804201; b) L. Chen, W. Xiang, S. Ouyang, H. Wu, Q. Xia, J. Ma, Y. Zeng, P. Lei, W. Xiao, S. Li, Y. Kuzyakov, *Land Degrad. Dev.* **2021**, *32*, 1164.

[5] a) D. Chen, Y. Zou, S. Wang, *Mater. Today Energy* **2019**, *12*, 250; b) H. Yi, M. Yan, D. Huang, G. Zeng, C. Lai, M. Li, X. Huo, L. Qin, S. Liu, X. Liu, B. Li, H. Wang, M. Shen, Y. Fu, X. Guo, *Appl. Catal., B* **2019**, *250*, 52; c) B. Li, C. Lai, G. Zeng, D. Huang, L. Qin, M. Zhang, M. Cheng, X. Liu, H. Yi, C. Zhou, F. Huang, S. Liu, Y. Fu, *Small* **2019**, *15*, 1804565; d) H. Yi, L. Qin, D. Huang, G. Zeng, C. Lai, X. Liu, B. Li, H. Wang, C. Zhou, F. Huang, S. Liu, X. Guo, *Chem. Eng. J.* **2019**, *358*, 480; e) M. Zhang, C. Lai, B. Li, D. Huang, G. Zeng, P. Xu, L. Qin, S. Liu, X. Liu, H. Yi, M. Li, C. Chu, Z. Chen, *J. Catal.* **2019**, *369*, 469; f) H. Yi, M. Jiang, D. Huang, G. Zeng, C. Lai, L. Qin, C. Zhou, B. Li, X. Liu, M. Cheng, W. Xue, P. Xu, C. Zhang, *J. Taiwan Inst. Chem. Eng.* **2018**, *93*, 184.

[6] a) L. Yang, L. Chen, D. Yang, X. Yu, H. Xue, L. Feng, *J. Power Sources* **2018**, *392*, 23; b) L. Yu, J. F. Yang, B. Y. Guan, Y. Lu, X. W. D. Lou, *Angew. Chem., Int. Ed. Engl.* **2018**, *57*, 172.

[7] G. Chen, T. Wang, J. Zhang, P. Liu, H. Sun, X. Zhuang, M. Chen, X. Feng, *Adv. Mater.* **2018**, *30*, 1706279.

[8] D. Zhou, Z. Cai, X. Lei, W. Tian, Y. Bi, Y. Jia, N. Han, T. Gao, Q. Zhang, Y. Kuang, J. Pan, X. Sun, X. Duan, *Adv. Energy Mater.* **2018**, *8*, 1701905.

[9] a) H. Xu, B. Wang, C. Shan, P. Xi, W. Liu, Y. Tang, *ACS Appl. Mater. Interfaces* **2018**, *10*, 6336; b) W. Ma, R. Ma, J. Wu, P. Sun, X. Liu, K. Zhou, T. Sasaki, *Nanoscale* **2016**, *8*, 10425; c) X. Long, J. Li, S. Xiao, K. Yan, Z. Wang, H. Chen, S. Yang, *Angew. Chem., Int. Ed. Engl.* **2014**, *53*, 7584; d) D. Zhou, S. Wang, Y. Jia, X. Xiong, H. Yang, S. Liu, J. Tang, J. Zhang, D. Liu, L. Zheng, Y. Kuang, X. Sun, B. Liu, *Angew. Chem. Int., Ed. Engl.* **2019**, *58*, 736.

[10] a) C. J. Heard, J. Cejka, M. Opanasenko, P. Nachtigall, G. Centi, S. Perathoner, *Adv. Mater.* **2019**, *31*, 1801712; b) H. Jin, C. Guo, X. Liu, J. Liu, A. Vasileff, Y. Jiao, Y. Zheng, S.-Z. Qiao, *Chem. Rev.* **2018**, *118*, 6337; c) C. Tan, X. Cao, X.-J. Wu, Q. He, J. Yang, X. Zhang, J. Chen, W. Zhao, S. Han, G.-H. Nam, M. Sindoro, H. Zhang, *Chem. Rev.* **2017**, *117*, 6225; d) X. Li, X. Hao, A. Abudula, G. Guan, *J. Mater. Chem. A* **2016**, *4*, 11973.

[11] G. Fan, F. Li, D. G. Evans, X. Duan, *Chem. Soc. Rev.* **2014**, *43*, 7040.

[12] X. Long, Z. L. Wang, S. Xiao, Y. M. An, S. H. Yang, *Mater. Today* **2016**, *19*, 213.

[13] Z. Wang, X. Long, S. Yang, *ACS Omega* **2018**, *3*, 16529.

[14] M. Ju, X. Wang, X. Long, S. Yang, *CrystEngComm* **2020**, *22*, 1531.

[15] a) R. Patel, J. T. Park, M. Patel, J. K. Dash, E. B. Gowd, R. Karpoormath, A. Mishra, J. Kwak, J. H. Kim, *J. Mater. Chem. A* **2018**, *6*, 12; b) X. Long, W. Qiu, Z. Wang, Y. Wang, S. Yang, *Mater. Today Chem.* **2019**, *11*, 16.

[16] L. Lv, Z. X. Yang, K. Chen, C. D. Wang, Y. J. Xiong, *Adv. Energy Mater.* **2019**, *9*, 1803358.

[17] a) C. Jing, B. Dong, Y. Zhang, *Energy Environ. Mater.* **2020**, *3*, 346; b) B. M. Hunter, W. Hieringer, J. R. Winkler, H. B. Gray, A. M. Müller, *Energy Environ. Sci.* **2016**, *9*, 1734.

[18] H. Zhang, M. Usman Tahir, X. Yan, X. Liu, X. Su, L. Zhang, *Chem. Eng. J.* **2019**, *368*, 905.

[19] M. Zeng, J. Wu, Z. Li, H. Wu, J. Wang, H. Wang, L. He, X. Yang, *ACS Sustainable Chem. Eng.* **2019**, *7*, 4777.

[20] H. Zhong, X. Cheng, H. Xu, L. Li, D. Li, P. Tang, N. Alonso-Vante, Y. Feng, *Electrochim. Acta* **2017**, *258*, 554.

[21] Z. Cai, X. Bu, P. Wang, J. C. Ho, J. Yang, X. Wang, *J. Mater. Chem. A* **2019**, *7*, 5069.

[22] X. Chia, M. Pumera, *Nat. Catal.* **2018**, *1*, 909.

[23] J. Yang, C. Yu, C. Hu, M. Wang, S. Li, H. Huang, K. Bustillo, X. Han, C. Zhao, W. Guo, Z. Zeng, H. Zheng, J. Qiu, *Adv. Funct. Mater.* **2018**, *28*, 1803272.

[24] a) J. Kibsgaard, Z. Chen, B. N. Reinecke, T. F. Jaramillo, *Nat. Mater.* **2012**, *11*, 963; b) L. Mohapatra, K. Parida, *J. Mater. Chem. A* **2016**, *4*, 10744; c) A. Shen, Y. Zou, Q. Wang, R. A. Dryfe, X. Huang, S. Dou, L. Dai, S. Wang, *Angew. Chem., Int. Ed. Engl.* **2014**, *53*, 10804.

[25] C. Yu, X. Han, Z. Liu, C. Zhao, H. Huang, J. Yang, Y. Niu, J. Qiu, *Carbon* **2018**, *126*, 437.

[26] Y. Wang, C. Xie, Z. Zhang, D. Liu, R. Chen, S. Wang, *Adv. Funct. Mater.* **2018**, *28*, 1703363.

[27] D. Zhou, X. Xiong, Z. Cai, N. Han, Y. Jia, Q. Xie, X. Duan, T. Xie, X. Zheng, X. Sun, X. Duan, *Small Methods* **2018**, *2*, 1800083.

[28] Y. Zhao, X. Zhang, X. Jia, G. I. N. Waterhouse, R. Shi, X. Zhang, F. Zhan, Y. Tao, L.-Z. Wu, C.-H. Tung, D. O'Hare, T. Zhang, *Adv. Energy Mater.* **2018**, *8*, 1703585.

[29] R. Gao, D. Yan, *Nano Res.* **2018**, *11*, 1883.

[30] S. Chen, Z. Kang, X. Hu, X. Zhang, H. Wang, J. Xie, X. Zheng, W. Yan, B. Pan, Y. Xie, *Adv. Mater.* **2017**, *29*, 1701687.

[31] J. Zhang, C. Dong, Z. Wang, H. Gao, J. Niu, Z. Peng, Z. Zhang, *Small Methods* **2019**, *3*, 1800286.

[32] H.-F. Wang, C. Tang, B.-Q. Li, Q. Zhang, *Inorg. Chem. Front.* **2018**, *5*, 521.

[33] L. Huang, R. Chen, C. Xie, C. Chen, Y. Wang, Y. Zeng, D. Chen, S. Wang, *Nanoscale* **2018**, *10*, 13638.

[34] D. J. Zhou, Z. Cai, Y. M. Bi, W. L. Tian, M. Luo, Q. Zhang, Q. Zhang, Q. X. Xie, J. D. Wang, Y. P. Li, Y. Kuang, X. Duan, M. Bajdich, S. Siahrostami, X. M. Sun, *Nano Res.* **2018**, *11*, 1358.

[35] B. M. Hunter, J. D. Blakemore, M. Deimund, H. B. Gray, J. R. Winkler, A. M. Muller, *J. Am. Chem. Soc.* **2014**, *136*, 13118.

[36] a) T. Zhan, Y. Song, Q. Yang, W. Hou, *Chem. Eng. J.* **2016**, *306*, 1143; b) X. Pang, M. Sun, X. Ma, W. Hou, *J. Solid State Chem.* **2014**, *210*, 111.

[37] D. Sarkar, C. K. Ghosh, S. Mukherjee, K. K. Chattopadhyay, *ACS Appl. Mater. Interfaces* **2013**, *5*, 331.

[38] a) B. R. Venugopal, C. Shivakumara, M. Rajamathi, *J. Colloid Interface Sci.* **2006**, *294*, 234; b) S. O'Leary, D. O'Hare, G. Seeley, *Chem. Commun.* **2002**, *14*, 1506; c) U. Unal, *J. Solid State Chem.* **2007**, *180*, 2525; d) C. A. Antonyraj, P. Koilraj, S. Kannan, *Chem. Commun.* **2010**, *46*, 1902.

[39] a) M. Jobbagy, A. E. Regazzoni, *J. Colloid Interface Sci.* **2004**, *275*, 345; b) V. V. Naik, S. Vasudevan, *J. Phys. Chem. C* **2011**, *115*, 8221.

[40] N. Mao, C. H. Zhou, D. S. Tong, W. H. Yu, C. X. Cynthia Lin, *Appl. Clay Sci.* **2017**, *144*, 60.

[41] G. V. Manohara, D. A. Kunz, P. V. Kamath, W. Milius, J. Breu, *Langmuir* **2010**, *26*, 15586.

[42] S. Dou, L. Tao, R. Wang, S. El Hankari, R. Chen, S. Wang, *Adv. Mater.* **2018**, *30*, 1705850.

[43] a) W. Zhong, J. Chen, P. Zhang, L. Deng, L. Yao, X. Ren, Y. Li, H. Mi, L. Sun, *J. Mater. Chem. A* **2017**, *5*, 16605; b) L. Tao, X. Duan, C. Wang, X. Duan, S. Wang, *Chem. Commun.* **2015**, *51*, 7470; c) Y. Wang, Y. Zhang, Z. Liu, C. Xie, S. Feng, D. Liu, M. Shao, S. Wang, *Angew. Chem., Int. Ed. Engl.* **2017**, *56*, 5867.

[44] a) T. Faraz, M. van Drunen, H. C. Knoops, A. Mallikarjunan, I. Buchanan, D. M. Hausmann, J. Henri, W. M. Kessels, *ACS Appl. Mater. Interfaces* **2017**, *9*, 1858; b) T. H. Chang, P. Y. Hsieh, S. Kunuku, S. C. Lou, D. Manoharan, K. C. Leou, I. N. Lin, N. H. Tai, *ACS Appl. Mater. Interfaces* **2015**, *7*, 27526; c) Z. Ma, C. Prawoto, Z. Ahmed, Y. Xiao, L. Zhang, C. Zhou, M. Chan, *J. Mater. Chem. C* **2019**, *7*, 6273.

[45] a) K. N. Dinh, X. Sun, Z. Dai, Y. Zheng, P. Zheng, J. Yang, J. Xu, Z. Wang, Q. Yan, *Nano Energy* **2018**, *54*, 82; b) S. Shaw, J. L. Colaux, J. L. Hay, F. C. Peiris, L. Cademartiri, *Adv. Mater.* **2016**, *28*, 8900; c) C. Petridis, D. Konios, M. M. Stylianakis, G. Kakavelakis,

M. Sygletou, K. Savva, P. Tzourmpakis, M. Krassas, N. Vaenas, E. Stratakis, E. Kymakis, *Nanoscale Horiz.* **2016**, *1*, 375.

[46] a) M. He, H. P. Zhou, G. Q. Ding, Z. D. Zhang, X. Ye, D. Cai, M. Q. Wu, *Carbon* **2019**, *146*, 194; b) B. Groven, M. Heyne, A. Nalin Mehta, H. Bender, T. Nuytten, J. Meersschaut, T. Conard, P. Verdonck, S. Van Elshocht, W. Vandervorst, S. De Gendt, M. Heyns, I. Radu, M. Caymax, A. Delabie, *Chem. Mater.* **2017**, *29*, 2927; c) J. M. Park, S. J. Jang, S. I. Lee, W. J. Lee, *ACS Appl. Mater. Interfaces* **2018**, *10*, 9155.

[47] a) S. Dou, L. Tao, J. Huo, S. Wang, L. Dai, *Energy Environ. Sci.* **2016**, *9*, 1320; b) Z. Jin, Z. Cai, X. Chen, D. Wei, *Nano Res.* **2018**, *11*, 4923.

[48] R. Limpens, G. F. Pach, N. R. Neale, *Chem. Mater.* **2019**, *31*, 4426.

[49] a) R. Liu, Y. Wang, D. Liu, Y. Zou, S. Wang, *Adv. Mater.* **2017**, 29; b) S. Chae, M. A. Bratescu, N. Saito, *J. Phys. Chem. C* **2017**, *121*, 23793; c) G. Panomsuwan, N. Saito, T. Ishizaki, *J. Mater. Chem. A* **2015**, *3*, 9972; d) B. Cui, B. Hu, J. Liu, M. Wang, Y. Song, K. Tian, Z. Zhang, L. He, *ACS Appl. Mater. Interfaces* **2018**, *10*, 23858.

[50] Y. Liu, M. Zhang, D. Hu, R. Li, K. Hu, K. Yan, *ACS Appl. Energy Mater.* **2019**, *2*, 1162.

[51] a) W. Lv, Q. Mei, H. Fu, J. Xiao, M. Du, Q. Zheng, *J. Mater. Chem. A* **2017**, *5*, 19079; b) M. Chatti, A. M. Glushenkov, T. Gengenbach, G. P. Knowles, T. C. Mendes, A. V. Ellis, L. Spiccia, R. K. Hocking, A. N. Simonov, *Sustainable Energy Fuels* **2018**, *2*, 1561; c) J. A. Carrasco, G. Abellán, E. Coronado, *J. Mater. Chem. C* **2018**, *6*, 1187; d) X. Jia, Y. Zhao, G. Chen, L. Shang, R. Shi, X. Kang, G. I. N. Waterhouse, L.-Z. Wu, C.-H. Tung, T. Zhang, *Adv. Energy Mater.* **2016**, *6*, 1502585; e) C. J. Wang, D. O'Hare, *J. Mater. Chem.* **2012**, *22*, 21125; f) Y. Zhao, X. Jia, G. Chen, L. Shang, G. I. Waterhouse, L. Z. Wu, C. H. Tung, D. O'Hare, T. Zhang, *J. Am. Chem. Soc.* **2016**, *138*, 6517.

[52] Y. Zhao, Q. Wang, T. Bian, H. Yu, H. Fan, C. Zhou, L. Z. Wu, C. H. Tung, D. O'Hare, T. Zhang, *Nanoscale* **2015**, *7*, 7168.

[53] a) H. Liu, Y. Wang, X. Lu, Y. Hu, G. Zhu, R. Chen, L. Ma, H. Zhu, Z. Tie, J. Liu, Z. Jin, *Nano Energy* **2017**, *35*, 350; b) J. Jiang, A. Zhang, L. Li, L. Ai, *J. Power Sources* **2015**, *278*, 445; c) L.-M. Cao, J.-W. Wang, D.-C. Zhong, T.-B. Lu, *J. Mater. Chem. A* **2018**, *6*, 3224.

[54] X. Long, S. Xiao, Z. Wang, X. Zheng, S. Yang, *Chem. Commun.* **2015**, *51*, 1120.

[55] Z. W. Gao, J. Y. Liu, X. M. Chen, X. L. Zheng, J. Mao, H. Liu, T. Ma, L. Li, W. C. Wang, X. W. Du, *Adv. Mater.* **2019**, *31*, 1804769.

[56] a) H. Yi, D. Huang, L. Qin, G. Zeng, C. Lai, M. Cheng, S. Ye, B. Song, X. Ren, X. Guo, *Appl. Catal., B* **2018**, *239*, 408; b) L. Li, C. Lai, F. Huang, M. Cheng, G. Zeng, D. Huang, B. Li, S. Liu, M. Zhang, L. Qin, M. Li, J. He, Y. Zhang, L. Chen, *Water Res.* **2019**, *160*, 238; c) C. Lai, F. Huang, G. Zeng, D. Huang, L. Qin, M. Cheng, C. Zhang, B. Li, H. Yi, S. Liu, L. Li, L. Chen, *Chemosphere* **2019**, *224*, 910; d) S. Y. Liu, C. Lai, B. S. Li, C. Zhang, M. M. Zhang, D. L. Huang, L. Qin, H. Yi, X. G. Liu, F. L. Huang, X. R. Zhou, L. Chen, *Chem. Eng. J.* **2020**, *384*, 10; e) X. Huo, Y. Yang, Q. Niu, Y. Zhu, G. Zeng, C. Lai, H. Yi, M. Li, Z. An, D. Huang, Y. Fu, B. Li, L. Li, M. Zhang, *Chem. Eng. J.* **2021**, *403*, 126363.

[57] D. Tang, J. Liu, X. Wu, R. Liu, X. Han, Y. Han, H. Huang, Y. Liu, Z. Kang, *ACS Appl. Mater. Interfaces* **2014**, *6*, 7918.

[58] Y. Wang, Z. Wang, Y. Rui, M. Li, *Biosens. Bioelectron.* **2015**, *64*, 57.

[59] C. Yu, Z. Liu, X. Han, H. Huang, C. Zhao, J. Yang, J. Qiu, *Carbon* **2016**, *110*, 1.

[60] F. Yan, D. Guo, J. Kang, L. Liu, C. Zhu, P. Gao, X. Zhang, Y. Chen, *Electrochim. Acta* **2018**, *283*, 755.

[61] X. Zhu, C. Tang, H.-F. Wang, Q. Zhang, C. Yang, F. Wei, *J. Mater. Chem. A* **2015**, *3*, 24540.

[62] H. Liu, J. Zhou, C. Wu, C. Wang, Y. Zhang, D. Liu, Y. Lin, H. Jiang, L. Song, *ACS Sustainable Chem. Eng.* **2018**, *6*, 2911.

[63] X. Long, J. Li, S. Xiao, K. Yan, Z. Wang, H. Chen, S. Yang, *Angew. Chem., Int. Ed.* **2014**, *53*, 7584.

[64] X. Han, C. Yu, J. Yang, C. Zhao, H. Huang, Z. Liu, P. M. Ajayan, J. Qiu, *Adv. Mater. Interfaces* **2016**, *3*, 1500782.

[65] Y. Jia, L. Zhang, G. Gao, H. Chen, B. Wang, J. Zhou, M. T. Soo, M. Hong, X. Yan, G. Qian, J. Zou, A. Du, X. Yao, *Adv. Mater.* **2017**, *29*, 1700017.

[66] C. Tang, H. S. Wang, H. F. Wang, Q. Zhang, G. L. Tian, J. Q. Nie, F. Wei, *Adv. Mater.* **2015**, *27*, 4516.

[67] a) J. Ping, Y. Wang, Q. Lu, B. Chen, J. Chen, Y. Huang, Q. Ma, C. Tan, J. Yang, X. Cao, Z. Wang, J. Wu, Y. Ying, H. Zhang, *Adv. Mater.* **2016**, *28*, 7640; b) Y. Qian, T. An, E. Sarnello, Z. Liu, T. Li, D. Zhao, *ACS Appl. Energy Mater.* **2019**, *2*, 1784.

[68] a) M. Wang, Y. Yang, Z. Yang, L. Gu, Q. Chen, Y. Yu, *Adv. Sci.* **2017**, *4*, 1600468; b) Y. Liu, Z. Xiao, Y. Liu, L.-Z. Fan, *J. Mater. Chem. A* **2018**, *6*, 160; c) L. Qie, W. Chen, H. Xu, X. Xiong, Y. Jiang, F. Zou, X. Hu, Y. Xin, Z. Zhang, Y. Huang, *Energy Environ. Sci.* **2013**, *6*, 2497.

[69] Q. Wang, L. Shang, R. Shi, X. Zhang, Y. Zhao, G. I. N. Waterhouse, L.-Z. Wu, C.-H. Tung, T. Zhang, *Adv. Energy Mater.* **2017**, *7*, 1700467.

[70] L. Chen, Y. Zhang, D. Li, Y. Wang, C. Duan, *J. Mater. Chem. A* **2018**, *6*, 18378.

[71] P. Zhou, Y. Wang, C. Xie, C. Chen, H. Liu, R. Chen, J. Huo, S. Wang, *Chem. Commun.* **2017**, *53*, 11778.

[72] Z. Guo, W. Ye, X. Fang, J. Wan, Y. Ye, Y. Dong, D. Cao, D. Yan, *Inorg. Chem. Front.* **2019**, *6*, 687.

[73] Q. Xie, Z. Cai, P. Li, D. Zhou, Y. Bi, X. Xiong, E. Hu, Y. Li, Y. Kuang, X. Sun, *Nano Res.* **2018**, *11*, 4524.

[74] Y.-S. Xie, Z. Wang, M. Ju, X. Long, S. Yang, *Chem. Sci.* **2019**, *10*, 8354.

[75] a) J. Huang, T. Lei, X. Wei, X. Liu, T. Liu, D. Cao, J. Yin, G. Wang, *J. Power Sources* **2013**, *232*, 370; b) J. Jiang, F. Sun, S. Zhou, W. Hu, H. Zhang, J. Dong, Z. Jiang, J. Zhao, J. Li, W. Yan, M. Wang, *Nat. Commun.* **2018**, *9*, 2885; c) V. Butera, M. Caspary Toroker, *J. Phys. Chem. C* **2016**, *120*, 12344.

[76] Q. Zhou, Y. Chen, G. Zhao, Y. Lin, Z. Yu, X. Xu, X. Wang, H. K. Liu, W. Sun, S. X. Dou, *ACS Catal.* **2018**, *8*, 5382.

[77] L. Hui, Y. Xue, B. Huang, H. Yu, C. Zhang, D. Zhang, D. Jia, Y. Zhao, Y. Li, H. Liu, Y. Li, *Nat. Commun.* **2018**, *9*, 5309.

[78] A. C. Thenuwara, N. H. Attanayake, J. Yu, J. P. Perdew, E. J. Elzinga, Q. Yan, D. R. Strongin, *J. Phys. Chem. B* **2018**, *122*, 847.

[79] D. Zhou, Z. Cai, Y. Jia, X. Xiong, Q. Xie, S. Wang, Y. Zhang, W. Liu, H. Duan, X. Sun, *Nanoscale Horiz.* **2018**, *3*, 532.

[80] P. Li, X. Duan, Y. Kuang, Y. Li, G. Zhang, W. Liu, X. Sun, *Adv. Energy Mater.* **2018**, *8*, 1703341.

[81] L. Qian, W. Chen, M. Liu, Q. Jia, D. Xiao, *ChemElectroChem* **2016**, *3*, 950.

[82] S. Yin, W. Tu, Y. Sheng, Y. Du, M. Kraft, A. Borgna, R. Xu, *Adv. Mater.* **2018**, *30*, 1705106.

[83] Y. Hu, G. Luo, L. Wang, X. Liu, Y. Qu, Y. Zhou, F. Zhou, Z. Li, Y. Li, T. Yao, C. Xiong, B. Yang, Z. Yu, Y. Wu, *Adv. Energy Mater.* **2021**, *11*, 2002816.

[84] a) T. D. Thanh, J. Balamurugan, N. T. Tuan, H. Jeong, S. H. Lee, N. H. Kim, J. H. Lee, *Biosens. Bioelectron.* **2017**, *89*, 750; b) V. C. Anitha, R. Zazpe, M. Krbal, J. Yoo, H. Sopha, J. Prikryl, G. Cha, S. Slang, P. Schmuki, J. M. Macak, *J. Catal.* **2018**, *365*, 86; c) Y. Fu, L. Qin, D. Huang, G. Zeng, C. Lai, B. Li, J. He, H. Yi, M. Zhang, M. Cheng, X. Wen, *Appl. Catal., B* **2019**, *255*, 117740.

[85] J. Zhang, J. Liu, L. Xi, Y. Yu, N. Chen, S. Sun, W. Wang, K. M. Lange, B. Zhang, *J. Am. Chem. Soc.* **2018**, *140*, 3876.

[86] a) L. Hu, M. Li, X. Wei, H. Wang, Y. Wu, J. Wen, W. Gu, C. Zhu, *Chem. Eng. J.* **2020**, *398*, 125605; b) L. Wan, D. Chen, J. Liu, Y. Zhang, J. Chen, M. Xie, C. Du, *J. Power Sources* **2020**, *465*, 228293; c) S. Bai, H. Chu, X. Xiang, R. Luo, J. He, A. Chen, *Chem. Eng. J.* **2018**, *350*, 148; d) B. L. Yue, D. Jia, J. Tang, A. Zhang, F. Liu, T. Chen, C. Barrow, W. Yang, J. Liu, *J. Colloid Interface Sci.* **2020**, *560*, 237.

[87] S. Anantharaj, K. Karthick, M. Venkatesh, T. V. S. V. Simha, A. S. Salunke, L. Ma, H. Liang, S. Kundu, *Nano Energy* **2017**, *39*, 30.

[88] X. Deng, J. Huang, F. Chen, H. Wan, Y. Lin, X. Xu, R. Ma, T. Sasaki, *Dalton Trans.* **2019**, *48*, 1084.

[89] J. Guo, J. Sun, Y. Sun, Q. Liu, X. Zhang, *Mater. Chem. Front.* **2019**, *3*, 842.

[90] F. Song, X. Hu, *Nat. Commun.* **2014**, *5*, 4477.

[91] F. Song, X. Hu, *J. Am. Chem. Soc.* **2014**, *136*, 16481.

[92] a) Y. Lin, X. Xie, X. Wang, B. Zhang, C. Li, H. Wang, L. Wang, *Electrochim. Acta* **2017**, *246*, 406; b) X. Ge, C. D. Gu, X. L. Wang, J. P. Tu, *J. Mater. Chem. A* **2014**, *2*, 17066; c) C. Qiao, Y. Zhang, Y. Zhu, C. Cao, X. Bao, J. Xu, *J. Mater. Chem. A* **2015**, *3*, 6878; d) Y. Zhao, T. Sun, Q. Yin, J. Zhang, S. Zhang, J. Luo, H. Yan, L. Zheng, J. Han, M. Wei, *J. Mater. Chem. A* **2019**, *7*, 15371; e) X. Li, X. Hao, Z. Wang, A. Abudula, G. Guan, *J. Power Sources* **2017**, *347*, 193; f) A. Sumboja, J. Chen, Y. Zong, P. S. Lee, Z. Liu, *Nanoscale* **2017**, *9*, 774.

[93] L. Su, H. Du, C. Tang, K. Nan, J. Wu, C. Ming Li, *J. Colloid Interface Sci.* **2018**, *528*, 36.

[94] a) G. Shi, C. Yu, Z. Fan, J. Li, M. Yuan, *ACS Appl. Mater. Interfaces* **2019**, *11*, 2662; b) Y. Zheng, J. Qiao, J. Yuan, J. Shen, A.-j. Wang, P. Gong, X. Weng, L. Niu, *Electrochim. Acta* **2018**, *282*, 735; c) G. Jia, Y. Hu, Q. Qian, Y. Yao, S. Zhang, Z. Li, Z. Zou, *ACS Appl. Mater. Interfaces* **2016**, *8*, 14527.

[95] J. Li, X. Gao, Z. Li, J. H. Wang, L. Zhu, C. Yin, Y. Wang, X. B. Li, Z. Liu, J. Zhang, C. H. Tung, L. Z. Wu, *Adv. Funct. Mater.* **2019**, *29*, 1808079.

[96] T. Zhan, Y. Zhang, X. Liu, S. Lu, W. Hou, *J. Power Sources* **2016**, *333*, 53.

[97] a) K. Xiao, L. Zhou, M. Shao, M. Wei, *J. Mater. Chem. A* **2018**, *6*, 7585; b) Z. Wu, Z. Zou, J. Huang, F. Gao, *ACS Appl. Mater. Interfaces* **2018**, *10*, 26283.

[98] X. Wang, Y. Yang, L. Diao, Y. Tang, F. He, E. Liu, C. He, C. Shi, J. Li, J. Sha, S. Ji, P. Zhang, L. Ma, N. Zhao, *ACS Appl. Mater. Interfaces* **2018**, *10*, 35145.

[99] a) T. Zhang, M.-Y. Wu, D.-Y. Yan, J. Mao, H. Liu, W.-B. Hu, X.-W. Du, T. Ling, S.-Z. Qiao, *Nano Energy* **2018**, *43*, 103; b) J. Huang, J. Chen, T. Yao, J. He, S. Jiang, Z. Sun, Q. Liu, W. Cheng, F. Hu, Y. Jiang, Z. Pan, S. Wei, *Angew. Chem., Int. Ed. Engl.* **2015**, *54*, 8722; c) J. Huang, Q. Shang, Y. Huang, F. Tang, Q. Zhang, Q. Liu, S. Jiang, F. Hu, W. Liu, Y. Luo, T. Yao, Y. Jiang, Z. Pan, Z. Sun, S. Wei, *Angew. Chem., Int. Ed. Engl.* **2016**, *55*, 2137.

[100] a) L. Yu, H. Zhou, J. Sun, F. Qin, F. Yu, J. Bao, Y. Yu, S. Chen, Z. Ren, *Energy Environ. Sci.* **2017**, *10*, 1820; b) L. Yu, H. Zhou, J. Sun, F. Qin, D. Luo, L. Xie, F. Yu, J. Bao, Y. Li, Y. Yu, S. Chen, Z. Ren, *Nano Energy* **2017**, *41*, 327.

[101] Z. Wang, S. Zeng, W. Liu, X. Wang, Q. Li, Z. Zhao, F. Geng, *ACS Appl. Mater. Interfaces* **2017**, *9*, 1488.

[102] A. A. Ensafi, A. Nabiyan, M. Jafari-Asl, M. Dinari, H. Farrokhpour, B. Rezaei, *Energy* **2016**, *116*, 1087.

[103] Y. Yang, W. Zhang, Y. Xiao, Z. Shi, X. Cao, Y. Tang, Q. Gao, *Appl. Catal., B* **2019**, *242*, 132.

[104] a) Y. Zeng, Y. Wang, G. Huang, C. Chen, L. Huang, R. Chen, S. Wang, *Chem. Commun.* **2018**, *54*, 1465; b) L. Ma, Y. Hu, R. Chen, G. Zhu, T. Chen, H. Lv, Y. Wang, J. Liang, H. Liu, C. Yan, H. Zhu, Z. Tie, Z. Jin, J. Liu, *Nano Energy* **2016**, *24*, 139; c) J. Wang, T. Qiu, X. Chen, Y. Lu, W. Yang, *J. Power Sources* **2015**, *293*, 178; d) W. Zhang, Y. Zou, H. Liu, S. Chen, X. Wang, H. Zhang, X. She, D. Yang, *Nano Energy* **2019**, *56*, 813.

[105] P. F. Liu, S. Yang, B. Zhang, H. G. Yang, *ACS Appl. Mater. Interfaces* **2016**, *8*, 34474.

[106] a) K. B. Ibrahim, W.-N. Su, M.-C. Tsai, S. A. Chala, A. W. Kahsay, M.-H. Yeh, H.-M. Chen, A. D. Duma, H. Dai, B.-J. Hwang, *Nano Energy* **2018**, *47*, 309; b) D. Kubo, K. Tadanaga, A. Hayashi, M. Tatsumisago, *J. Mater. Chem. A* **2013**, *1*, 6804; c) L. Wang, C. Lin, D. Huang, F. Zhang, M. Wang, J. Jin, *ACS Appl. Mater. Interfaces* **2014**, *6*, 10172.

[107] a) W. Wang, Y. Liu, J. Li, J. Luo, L. Fu, S. Chen, *J. Mater. Chem. A* **2018**, *6*, 14299; b) M. F. P. Duarte, I. M. Rocha, J. L. Figueiredo, C. Freire, M. F. R. Pereira, *Catal. Today* **2018**, *301*, 17.

[108] Y. Wang, G. I. N. Waterhouse, L. Shang, T. Zhang, *Adv. Energy Mater.* **2020,** https://doi.org/10.1002/aenm.202003323.

[109] J. H. Huang, J. X. Chen, C. L. Fu, P. W. Cai, Y. Li, L. L. Cao, W. Liu, P. Yu, S. Q. Wei, Z. H. Wen, J. H. Li, *ChemSusChem* **2020**, *13*, 1496.

[110] a) D.-H. Nam, P. De Luna, A. Rosas-Hernández, A. Thevenon, F. Li, T. Agapie, J. C. Peters, O. Shekhah, M. Eddaoudi, E. H. Sargent, *Nat. Mater.* **2020**, *19*, 266; b) F. Naseem, P. L. Lu, J. P. Zeng, Z. Y. Lu, Y. H. Ng, H. T. Zhao, Y. P. Du, Z. Y. Yin, *ACS Nano* **2020**, *14*, 7734.

[111] W. T. Li, P. F. Hou, Z. Wang, P. Kang, *Sustainable Energy Fuels* **2019**, *3*, 1455.

[112] M. Arif, G. Yasin, L. Luo, W. Ye, M. A. Mushtaq, X. Fang, X. Xiang, S. Ji, D. Yan, *Appl. Catal., B* **2020**, *265*, 118559.

[113] W.-J. Liu, L. Dang, Z. Xu, H.-Q. Yu, S. Jin, G. W. Huber, *ACS Catal.* **2018**, *8*, 5533.

[114] X. Deng, X. Kang, M. Li, K. Xiang, C. Wang, Z. Guo, J. Zhang, X.-Z. Fu, J.-L. Luo, *J. Mater. Chem. A* **2020**, *8*, 1138.

[115] M. Zhang, Y. Liu, B. Liu, Z. Chen, H. Xu, K. Yan, *ACS Catal.* **2020**, *10*, 5179.

[116] L. Zhou, M. F. Shao, C. Zhang, J. W. Zhao, S. He, D. M. Rao, M. Wei, D. G. Evans, X. Duan, *Adv. Mater.* **2017**, *29*, 8.

[117] S. O. Ganiyu, T. X. H. Le, M. Bechelany, N. Oturan, S. Papirio, G. Esposito, E. van Hullebusch, M. Cretin, M. A. Oturan, *Chem. Eng. J.* **2018**, *350*, 844.

[118] G. Karim-Nezhad, S. Pashazadeh, A. Pashazadeh, *Chin. J. Catal.* **2012**, *33*, 1809.

[119] S. Gamil, W. M. A. El Rouby, M. Antuch, I. T. Zedan, *RSC Adv.* **2019**, *9*, 13503.

[120] X. Y. Lu, H. R. Xue, H. Gong, M. J. Bai, D. M. Tang, R. Z. Ma, T. Sasaki, *Nano-Micro Lett.* **2020**, *12*, 86.

[121] H. Sun, L. Chen, Y. Lian, W. Yang, L. Lin, Y. Chen, J. Xu, D. Wang, X. Yang, M. H. Rummerli, J. Guo, J. Zhong, Z. Deng, Y. Jiao, Y. Peng, S. Qiao, *Adv. Mater.* **2020**, *32*, 2006784.

[122] K. Fan, Z. H. Li, Y. J. Song, W. F. Xie, M. F. Shao, M. Wei, *Adv. Funct. Mater.* **2020**, 2008064, https://doi.org/10.1002/adfm.202008064.

[123] L. Xu, X. Zhai, W. Lin, X. Chen, F. Li, W. Yang, *Electrochim. Acta* **2019**, *318*, 590.

[124] a) X. Lu, C. Zhao, *Nat. Commun.* **2015**, *6*, 6616; b) W. Xu, Z. Lu, X. Sun, L. Jiang, X. Duan, *Acc. Chem. Res.* **2018**, *51*, 1590.

Huan Yi is currently pursuing her Ph.D. under the supervision of Prof. Guangming Zeng in College of Environmental Science and Engineering, Hunan University, China. Her current research interests focus on functional nanomaterials science.

Shiyu Liu received her master's degree in 2019 in Hunan University, Changsha, China. She is currently pursuing her Ph.D. under the supervision of Prof. Cui Lai in the College of Environmental Science and Engineering, Hunan University. Her current research interests focus on the synthesis of carbon materials and their applications in persulfate-based advanced oxidation processes for environmental remediation.

Cui Lai graduated from the College of Environmental Science and Engineering of Hunan University in 2013 and received her Ph.D. degree in Environmental Science. She joined Professor Guangming Zeng's group at Hunan University after completing her Ph.D. degree. Her main research interests are the development and environmental application of functional nanomaterials.

Guangming Zeng has taught courses and performed research on Environmental Science and Health at Hunan University since 1988. He is one of the 2017 Highly Cited Researchers in the world issued by Clarivate Analytics. His honors include the National Science and Technology Progress Awards of China (the Second Award), National Technology Invention Awards of China (the Second Award), and a Lifetime Achievement Award of Changjiang Scholars. His current research interests focus on the synthesis and application of functional nanomaterials in the environment and energy field.